

## Sudden solar wind dynamic pressure enhancements and dayside detached auroras: IMAGE and DMSP observations

Y. Zhang and L. J. Paxton

Johns Hopkins University Applied Physics Laboratory, Laurel, Maryland, USA

T. J. Immel, H. U. Frey, and S. B. Mende

Space Science Laboratory, University of California, Berkeley, California, USA

Received 27 February 2002; revised 7 June 2002; accepted 11 June 2002; published 24 December 2002.

[1] Dayside detached auroras (DDA) refer to auroras observed separate from the equatorward edge of the main oval on the dayside. They are studied here using IMAGE FUV and DMSP particle data. Occurrence of these DDA appears to be correlated with sudden solar wind dynamic pressure enhancements and northward interplanetary magnetic field, as monitored by the Wind satellite. They are usually very dynamic and short-lived with a lifetime of the order of 10 minutes. Out of the three FUV instrument channels on IMAGE, DDA are best detected by the IMAGE FUV SI-12 instrument, which measures intensities of the Doppler red-shifted Hydrogen Lyman Alpha line. This indicates that energetic proton precipitation is the major component. Simultaneous DMSP particle observations confirm that energetic protons (>10 keV) in the dayside inner magnetosphere are the primary source of those DDA detected by the SI-12 instrument. DMSP also detected significant electron fluxes associated with the DDA, but the electron precipitations have little or no contribution to the DDA intensities detected by the SI-12 instrument. Precipitations of energetic protons (electrons) which caused DDA could be explained by enhanced cyclotron instability which arose from adiabatic compression following sudden solar wind dynamic pressure enhancements. *INDEX TERMS:* 2704 Magnetospheric Physics: Auroral phenomena (2407); 2784 Magnetospheric Physics: Solar wind/magnetosphere interactions; 2716 Magnetospheric Physics: Energetic particles, precipitating; 2483 Ionosphere: Wave/particle interactions; *KEYWORDS:* aurora, dayside detached aurora, proton precipitation, solar wind pressure enhancement

**Citation:** Zhang, Y., L. J. Paxton, T. J. Immel, H. U. Frey, and S. B. Mende, Sudden solar wind dynamic pressure enhancements and dayside detached auroras: IMAGE and DMSP observations, *J. Geophys. Res.*, 107, 8001, doi:10.1029/2002JA009355, 2002. [printed on 108(A4), 2003]

### 1. Introduction

[2] Detached auroral arcs or patches at subauroral latitudes in the evening sector were first reported by *Moshupi et al.* [1977] and *Anger et al.* [1978] using photometer data from the ISIS-2 satellite. Ground radar measurements from Chatanika, Alaska show that the detached arcs were  $\sim 2^\circ$  wide in latitude and separated by  $\sim 3^\circ$  from the equatorward edge of the diffuse aurora [*Vondrak et al.*, 1983b]. The detached arcs were only observed in the dusk/evening sector between 1500 and 2100 MLT. *Wallis et al.* [1979] showed that detached arcs were the result of energetic electron precipitation from a residual plasma sheet. On the basis of ISIS-2 satellite measurement, *Vondrak et al.* [1983b] also reported energetic electron precipitation (>40 keV) in the detached arcs. Ground-based photometric and all-sky television measurements at 630 nm and 427.8 nm confirmed the satellite observations of detached arcs [*Vondrak et al.*, 1983a].

[3] More progress in the study of detached arcs has been achieved after launch of the IMAGE satellite [*Burch*, 2000].

*Immel et al.* [2002] report that proton precipitation is the major source for detached arcs in the dusk sector. Furthermore, detached arcs are not limited to the dusk side. IMAGE FUV SI-12 instruments also observe the detached arcs in dayside [*Fuselier et al.*, 2000, 2001]. These earlier and more recent studies indicate that both electron and proton precipitation is important in forming the detached arcs. However, there is a lack of simultaneous electron/proton particle observations associated with optical measurements. *Immel et al.* [2002] also showed that the detached arcs in the dusk sector developed from a separation of the duskside auroral oval. We report here observations of a new phenomenon, dayside detached auroras down to 60 MLAT by the IMAGE SI-12 instrument with simultaneous in situ precipitating particle detection by DMSP. These dayside detached auroras were well separated from the dayside auroral oval during their lifetime and were not necessarily in the form of arcs; they could have the shape of patches [*Zhang et al.*, 2001].

### 2. Data

[4] One of the IMAGE FUV spectrographic imaging instruments, SI-12, is designed to measure the brightness

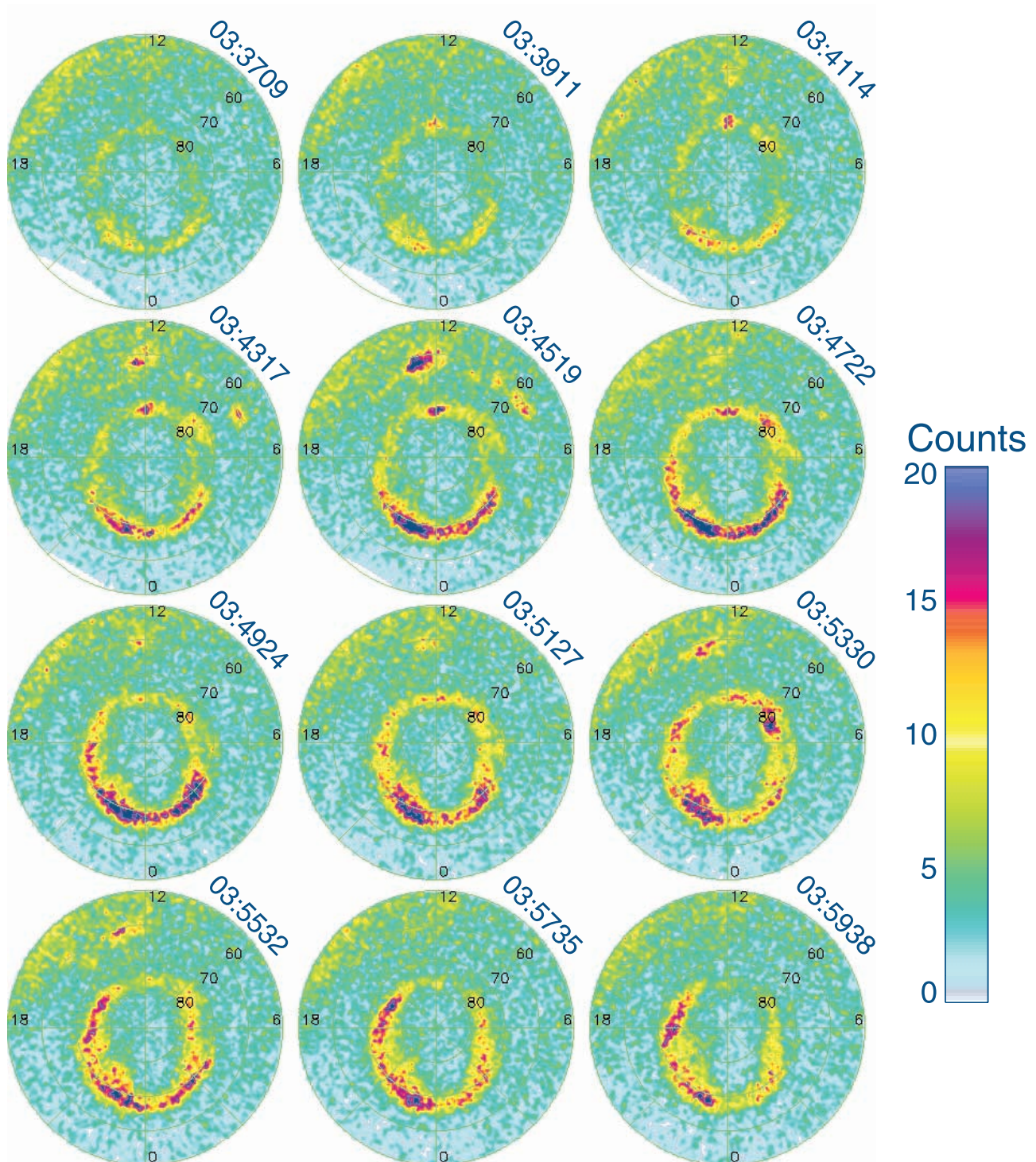


**Figure 1.** IMAGE FUV SI-12 images between 0337:09 and 0359:38 UT on 8 November 2000. The images are in magnetic coordinates with 0000, 0600, 1200, 1800 MLT at the bottom, right, top, and left, respectively. Magnetic latitudes at center and edge in each image are  $90^\circ$  and  $50^\circ$ , respectively.

of Doppler-shifted Lyman alpha line to monitor proton precipitation on a global scale with temporal resolution of 2 minutes and spatial resolution of  $\sim 300$  km [Mende *et al.*, 2000]. The SI-12 is a periodic narrow band system which utilizes a grill system to reject the geocoronal Lyman alpha emission at 121.56 nm while allowing a fraction of the

broad auroral Lyman alpha line profile through a transmission peak at  $\sim 121.8$  nm. Gerard *et al.* [2001] found the SI-12 mainly responds to energetic precipitating protons with energy from 1 to 20 keV. Contribution from the low-energy ( $< 0.3$  keV) precipitating protons is negligible. Gerard *et al.* [2001] also found a good agreement between the

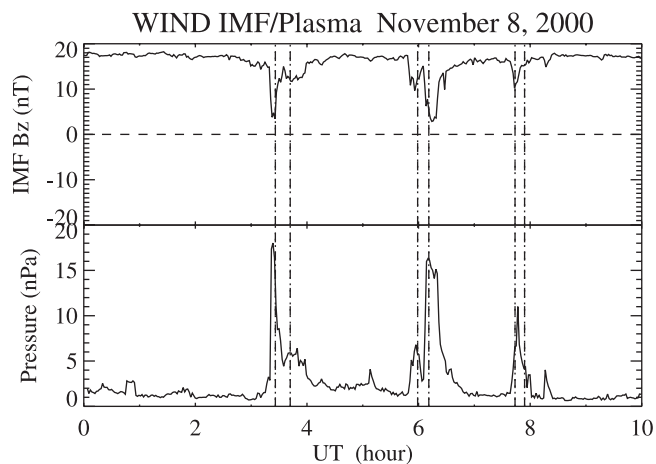


**Figure 2.** Plots of interplanetary magnetic field  $B_z$  and solar wind dynamic pressure from Wind satellite between 0000 and 1000 UT on 8 November 2000. Three major sudden pressure enhancements are seen between around 0320, 0600 UT, and 0740 UT. Each pair of vertical dash-dotted lines indicates starting and ending time (shifted-15 minutes owing to propagation of solar wind) of dayside detached auroras (DDA) or brightening of the auroral oval.

SI-12 and simultaneous FAST and DMSP observations at three different mean proton energies, 1.5 keV, 7 keV, and 15 keV. These studies indicate the SI-12 is an excellent instrument to monitor energetic proton precipitations.

[5] Particle detectors (SSJ/4) on DMSP satellites record precipitating fluxes of both electron and ion (mainly proton) simultaneously every second [Hardy *et al.*, 1984; Newell, 2000]. The detectors are orientated toward the zenith and produce a complete electron/ion spectrogram in the loss cone over 19 logarithmically spaced channels from 30 eV to 30 keV. Solar wind plasma and IMF conditions are continuously monitored by the Wind satellite. Data from the IMAGE, DMSP, and Wind satellites will be used to study the dayside detached aurora events on 8 November and 24 and 28 December 2000.

### 3. Cases on 8 November 2000

[6] Two DDA events were observed during one period of imaging between 0000 and 1000 UT on 8 November 2000. Figure 1 shows a history of the first DDA event recorded by IMAGE SI-12 instrument. The image at 0337 UT in Figure 1 shows a typical quiet auroral oval. A sudden brightening of dayside auroral oval at 1200 MLT (cusp region) was seen at 0339 UT. While intensity of the dayside auroral oval or cusp region continued to increase, a DDA at magnetic latitude (MLAT) between  $60^\circ$  and  $70^\circ$  appeared at 0341 UT. Meanwhile, the nightside auroral oval also brightened. Two minutes later, the DDA extended to the morning side around  $60^\circ$  MLAT. The DDA's intensity continued to increase until 0345 UT and then suddenly dropped to a very low level at 0347 UT. It disappeared around 0357 UT after another brightening between 0349 and 0355 UT. This gives a lifetime of 16 minutes for the DDA.

[7] Figure 2 shows a plot of IMF  $B_z$  and solar wind dynamic pressure ( $P_{sw} = N M_p V^2$ ) between 0000 and 1000

UT on 8 November 2000, where  $N$ ,  $M_p$ , and  $V$  are solar wind number density, proton mass, and solar wind speed, respectively. IMF  $B_z$  was strongly northward. A sudden pressure enhancement (from 3 to 18 nPa) was seen at 0320 UT. Two vertical dash-dotted lines between 0300 and 0400 UT show the DDA starting and ending time at 0326 and 0342 UT (0341 and 0357 UT shifted -15 minutes owing to solar wind propagation). The 15-minute delay was due to propagation of solar wind from the Wind position (77.0,  $-100.0$ , 30.1)  $R_E$  (GSM, around 0340 UT) at speed of  $-450$  km/s ( $V_x$ ) to the bow shock (around  $x = 15 R_E$ ) and from the bow shock to the magnetopause (around  $12 R_E$ ) at a reduced speed (assumed  $-350$  km/s). Using 6370 km as the Earth's radius, we have the total delay equal to  $(77 - 15) * 6370/450/60 + (15 - 12) * 6370/350/60 = 15.5$  minutes. We round it to 15 minutes. This indicates that the DDA occurred only  $\sim 6$  minutes after the sudden pressure enhancement arrived at the Earth's magnetopause. As the Wind satellite was far away ( $100 R_E$ ) from the GSM x-axis, it is necessary to verify the arriving time of solar wind pressure enhancement at the magnetopause. After examining the solar wind and IMF data from ACE and Geotail, We found that the front of the first enhancement was detected by ACE around 0245 UT at location of (219.78, 12.56,  $-26.22$ )  $R_E$  (GSM). The solar wind speed  $V_x$  was  $-445$  km/s at the time. Following the same procedure shown above, we have a delay of 49.7 minutes  $((219.78 - 15) * 6370/445/60 + (15 - 12) * 6370/350/60 = 49.7$  minutes). We assumed the same solar wind speed of 350 km/s in the magnetosheath. The arriving time at the magnetopause is  $0245\text{UT} + 49.7$  minutes = 0334.7 UT. This indicates the first DDA were observed  $\sim 6.3$  minutes later after the enhancement hit the dayside magnetopause. Furthermore, the Geotail was in the solar wind (11.77,  $-27.78$ , 1.26)  $R_E$  (GSE) but very close to the bow shock when it detected the first solar wind pressure enhancement at 0335 UT. The solar wind speed at the Geotail location was  $-450$  km/s ( $V_x$ ). As the Geotails's X position was at 11.77  $R_E$ , already the magnetopause X position, no time delay needs to be estimated (except the small delay  $< 0.5$  minutes due to the speed difference in the solar wind and the magnetosheath over a distance of 3  $R_E$ ). This shows that the first DDA was observed  $\sim 6$  minutes after the enhancement arrived at the magnetopause. All these estimations give almost the same arriving time of the enhancement. The difference is negligible, only 0.3 minutes or less. This confirms that the Wind data could be used to identify the enhancement arriving time. Thus the DDA was very likely caused by the sudden solar wind dynamic pressure enhancement. This idea is supported by the occurrence of a second DDA event just 2 hours later with similar variation in  $P_{sw}$ .

[8] The second DDA event was detected between 0614 and 0626 UT on 8 November 2000. Figure 3 shows a sequence of SI-12 images between 0610 and 0632 UT. The image at 0610 UT again shows a quiet auroral oval. Brightening of dayside and postnoon auroral oval was seen at 0612 UT, just 2 minutes before a bright DDA was detected at 0614 UT. Like the previous event, this DDA was again located between  $60^\circ$  and  $70^\circ$  MLAT. It quickly decayed in  $\sim 2$  minutes and disappeared around 0626 UT. This gives it a lifetime of 12 minutes. Brightening of nightside auroral oval was also seen  $\sim 4$  minutes after the DDA appeared at 0614 UT.

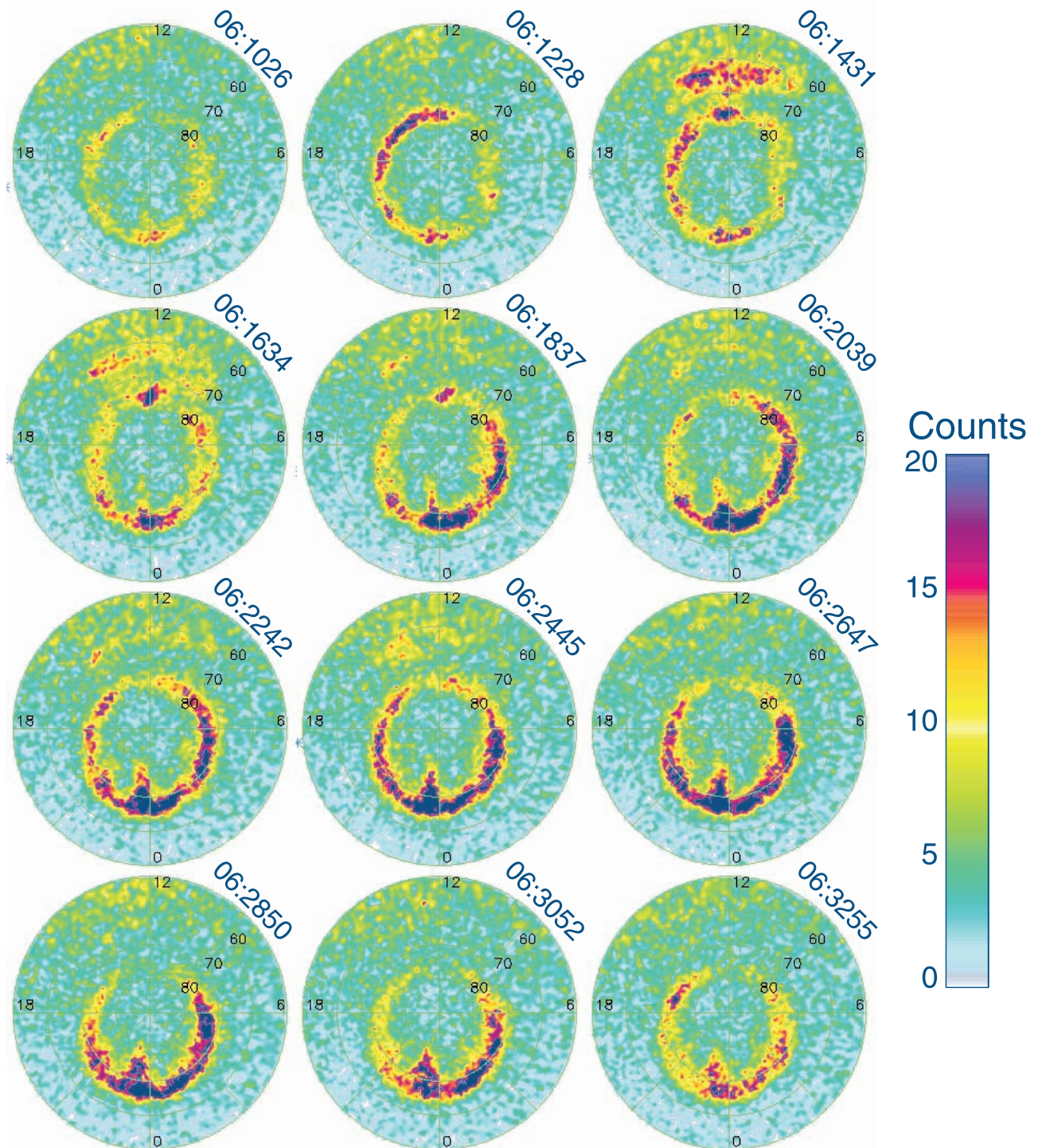


**Figure 3.** The same as Figure 1 but for images between 0610:26 and 0632:55 UT.

[9] The second sudden solar wind pressure enhancement (1 to 6 nPa) was observed at 0551 UT (see Figure 2) and followed by another pressure enhancement (3 to 16 nPa) at 0605 UT. As these two pressure enhancements came in such a rapid succession, their effects on DDA may not be distinct. The two vertical dash-dotted lines around 0600 UT are marked for the DDA starting and ending time at 0559 and 0611 UT, respectively (0614 and 0626 UT, shifted  $-15$  minutes). Thus the DDA occurred  $\sim 8$  minutes after the

pressure enhancement arrived at the magnetopause. This again suggests that the DDA was caused by sudden solar wind pressure enhancements.

[10] The third pressure enhancement between 0730 and 0800 UT (see Figure 2) is similar to the two which preceded. One would have expected to observe another DDA. However, the SI-12 instrument detected no such signature. Figure 4 shows a sequence of SI-12 images between 0734 and 0831 UT on 8 November 2000. What

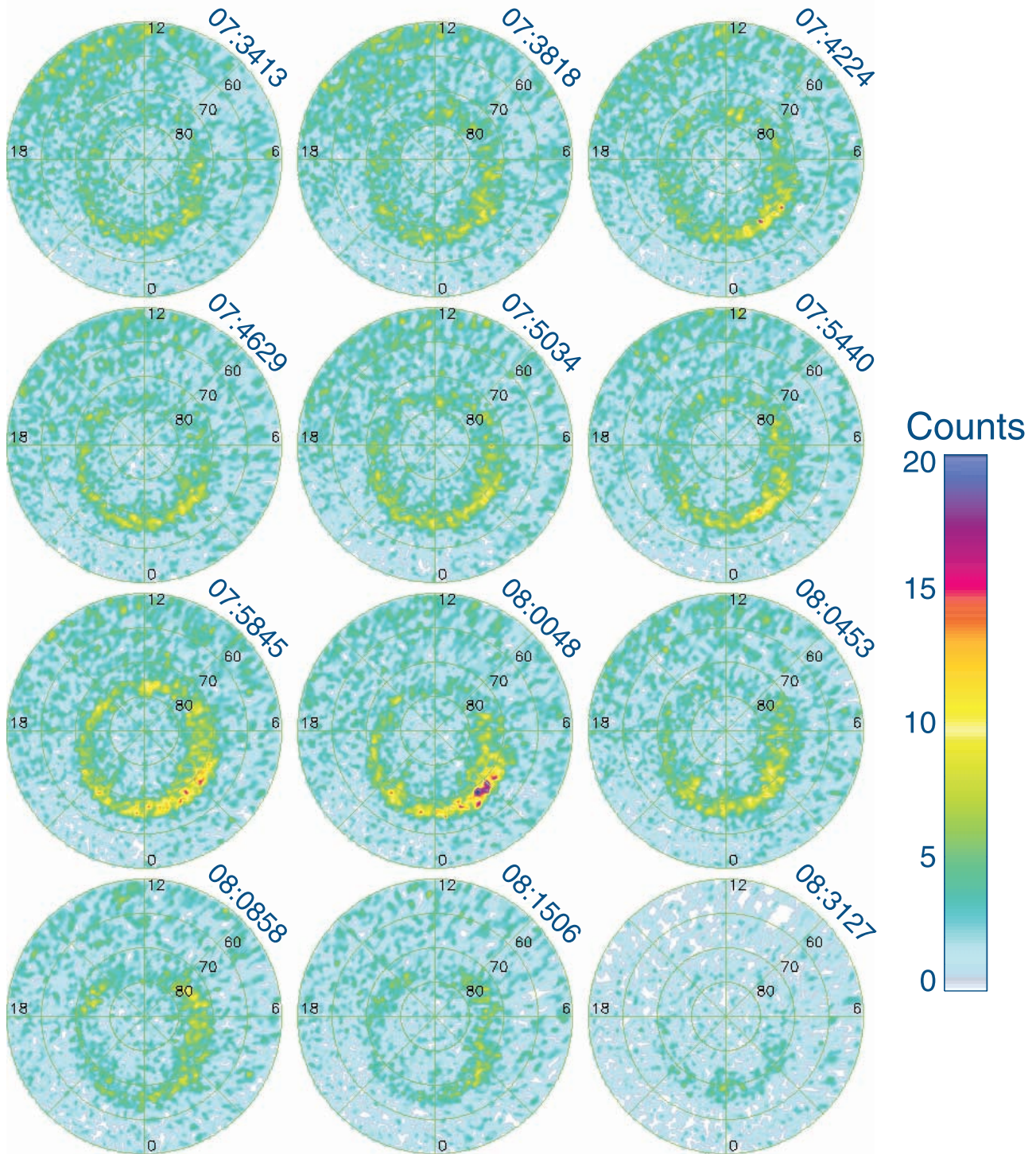


**Figure 4.** The same as Figure 1 but for images between 0734:13 and 0831:27 UT. Auroral oval brightening was seen between 0754 and 0804 UT.

we see is a very quiet auroral oval without DDA, except a brief brightening in cusp region at 0759 UT and nightside auroral oval between 0759 and 0809 UT. The last pair of vertical lines in Figure 2 shows starting and ending time of brighten auroral oval at 0744 and 0754 UT, respectively (0759 and 0809, shifted  $-15$  minutes). As the pressure enhancement arrived around 0739 UT, just 5 minutes before the brightening of auroral oval was seen, the brighten

auroral oval was very likely triggered by the pressure enhancement. Possible explanations for the lack of detectable DDAs will be discussed in section 6.

#### 4. Case on 24 December 2000

[11] Figure 5 shows six SI-12 images (roughly 2 minutes apart) starting at 2325:10 UT on 24 December 2000. A

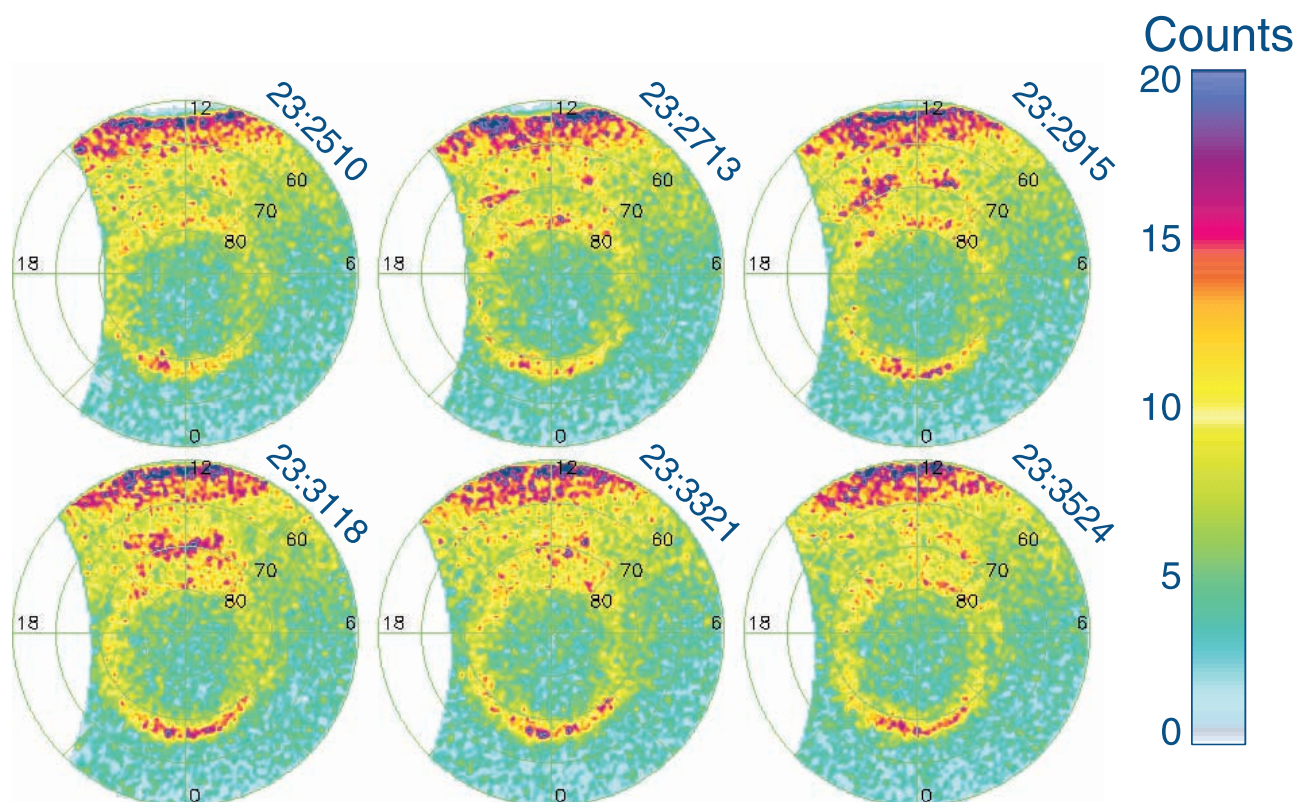


**Figure 5.** A sequence of six SI-12 images recorded at time from 2325:10 to 2335:24 UT on 24 December 2000. The color scale is from 0 to 20 counts. The persistent feature in dayside at magnetic latitudes below  $60^\circ$  was due to a leak from geocoronal emissions.

small and quiet auroral oval was seen at 2325:10 UT. Its noon and midnight locations were around  $78^\circ$  and  $67^\circ$  magnetic latitudes, respectively. By 2327:13 UT, two auroral emission patches brightened at latitudes just below  $70^\circ$  in prenoon and postnoon sectors. About 2 minutes later, these two DDA intensified and extended toward noon. They joined together at 2331:18 UT and formed a single extended arc. Then the DDA quickly decayed to an auroral patch in two minutes (at 2333:21 UT) and became a weak arc in the prenoon sector around 2335:24 UT. Thus the lifetime of this DDA is  $\sim 10$  minutes.

[12] Around 2335:24 UT, DMSP F15 satellite flew over the dayside auroral oval and the DDA. Figure 6a shows the SI-12 image at 2335:24 UT with a DMSP path (dark blue). The start (big square, 2330:00 UT) of the path was in the dayside polar cap. The satellite moved to lower latitudes in the 0900 MLT sector. The end point of the path was at 2335:54 UT. Before examining details of electron/proton fluxes we would like to note that the DDA also occurred after a sudden solar wind dynamic pressure enhancement. Figure 6b shows a plot of IMF  $B_z$  and solar wind dynamic pressure between 2000 and 2400 UT on 24 December 2000. The solar wind pressure suddenly increased from 2 nPa to 4 nPa around 2305 UT. The pressure reached its highest level of 7 nPa by 2330 UT. IMF  $B_z$  was strongly northward ( $>10$  nT) most of time, except for a short time of southward turning between 2311 and 2324 UT. IMAGE SI-12 instrument detected a few DDA events between 2314 UT, 24 December and 0111

UT, 25 December 2000 (not shown here). Those DDA come and go at locations near  $70^\circ$  MLAT and 1200 MLT every 10–20 minutes during the period. The first DDA, starting at 2314 UT, apparently followed the sudden solar wind pressure enhancement at 2305 UT. The solar wind speed was roughly constant at 375 km/s between 2000 and 2400 UT. As the Wind satellite was at (8.8, 237.6, 36.5)  $R_E$  (GSM) around 2300 UT, the time delay due to solar wind propagation from the Wind position to the magnetopause can be neglected, given that the dayside magnetopause was located between 10 and 15  $R_E$ . As the IMAGE SI-12 instrument measures only Doppler-shifted Lyman Alpha emissions, energetic proton precipitation must be a major component of the DDA. Figure 6c shows plots of the SI-12 image counts (thick line) and DMSP total ion (mainly proton) energy flux (thin line) along the DMSP path (see Figure 6a). Two major peaks (with counts above 10) are seen in the SI-12 intensities. They are due to the emissions from the dayside auroral oval and the DDA, respectively. The DMSP proton flux data show five major peaks. The first (around 2331:50) and last (around 2334:16) peaks appear to be well colocated with the dayside auroral oval and the DDA. The second (around 2332:33) and third (around 2333:00) proton flux peaks apparently associated with two small peaks in SI-12 (between the dayside oval and the DDA). The fourth major peak of proton flux (around 2333:40 UT) cannot be associated with any particular emissions. This may be due to highly dynamic nature of the DDA and that the

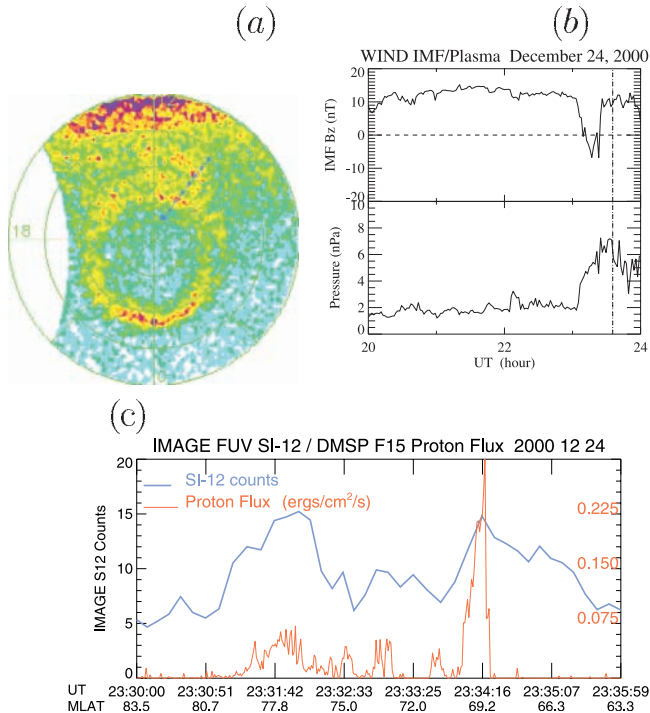


**Figure 6.** (a) IMAGE SI-12 image at 2335:24 UT, 24 December 2000. The dark blue dotted line is the track of DMSP F15 satellite between 2330 and 2336 UT, 24 December 2000. (b) Plot of IMF  $B_z$  and solar wind dynamic pressure between 2000 and 2400 UT on 24 December 2000. (c) Thick line: SI-12 counts (see scale on the left axis) along the DMSP F15 track in Figure 6a; Thin line: total ion (proton) energy flux in  $\text{ergs/cm}^2/\text{s}$  from DMSP F15 (see scale on the right axis).

times of the DMSP and SI-12 measurements were not exactly the same. Nevertheless, the DMSP and SI-12 observations give a fairly good agreement on location of the dayside auroral oval and the DDA. We also noticed that proton energy flux in the DDA is much higher than that in the dayside oval, but SI-12 counts for the DDA and the auroral oval are almost the same. Such difference is due to different response of the SI-12 to protons with various energies. *Gerard et al.* [2001] estimated the SI-12 counts as 36, 30, and 17 for a given proton energy flux of 1  $\text{ergs/cm}^2/\text{s}$  with difference energies at 2 keV, 8 keV, and 25 keV, respectively. The two major SI-12 peak counts (Figure 6c, corresponding to the dayside oval and the DDA) are about the same (14 count). By subtracting background level of 5 counts (for the oval) and 6 counts (for the DDA), we have net SI-12 counts of 9 and 8 due to proton precipitation. Figure 7 shows that the average proton energies are around 2 keV for the auroral oval and 20 keV for the DDA. Using the count rate from *Gerard et al.* [2001] at 2 keV and 25 keV, we estimated proton energy fluxes as 0.25 (9.0/36.0) and 0.47 (8.0/17.0)  $\text{ergs/cm}^2/\text{s}$ . These values are above but comparable to the DMSP measurements (0.075 and 0.30  $\text{ergs/cm}^2/\text{s}$  for the oval and DDA, respectively). Nevertheless, this simple estimation explains why higher (for the DDA) and lower (for the oval) proton energy fluxes produce nearly the

same SI-12 counts. A simulation is needed for detailed comparison between observed proton spectra and the SI-12 counts. It is beyond the scope of the current paper and will be addressed in a future paper. Note there is a weak electron flux (between 2 and 10 keV) associated with the DDA.

## 5. Case on 28 December 2000

[13] Another example of DDA was observed between 1323 and 1434 UT on 28 December 2000. It also apparently followed a sudden solar wind dynamic pressure enhancement at 1314 UT (see Figure 9b). There was a northward turning of IMF  $B_z$  associated with the pressure enhancement. The DDA was also very dynamic. Figure 8 shows four consecutive SI-12 images between 1359:54 and 1418:19 UT. The temporal resolution is worse than previous cases as a problem with spacecraft mass memory caused a partial loss of data. Initially, DDA could be identified at 1359:54 UT. Eight minutes later, patch-like DDA were apparent at and below  $70^\circ$  of magnetic latitude in the noon and postnoon sectors. The DDA was separated from the dayside auroral oval which stayed around  $76^\circ$  of magnetic latitudes. The DDA moved to the noon sector by 1410:08 UT and almost disappeared by 1418:19 UT. In this case the lifetime of the DDA is at least 10 minutes but not more than 18 minutes.

[14] Around 1410:08 UT, DMSP F15 satellite passed through the region of the auroral oval and the DDA. Figure 9a shows the SI-12 image at 1410:08 UT with the DMSP F15 path superimposed (dark blue line). We can see a quiet-time auroral oval and DDA at magnetic noon just below  $70^\circ$  MLAT. Figure 9b is a plot of Wind IMF  $B_z$  and solar wind plasma dynamic pressure from 1000 to 1600 UT. The time of the SI-12 image (1410:08) is marked by a vertical line. The Wind satellite was at location of (6.6, 242.2,  $-49.0$ )  $R_E$  (GSM). The solar wind speed was 370 km/s. Thus the time delay due to solar wind propagation from the Wind position to dayside magnetopause is negligible. Around 1314 UT the solar wind dynamic pressure suddenly increased from 2 to 5 nPa. This caused a DDA to appear around 1323 UT (not shown here). The DDA shown in Figure 9a was already at its later stage. Note the IMF  $B_z$  was northward during period of the DDA.

[15] SI-12 counts along the DMSP F15 track (see Figure 9a) and the corresponding DMSP proton energy flux were plotted together in Figure 9c. The thick line (SI-12 counts) clearly indicates three major peaks (from left to right with counts above 10). The peaks were due to emissions from the duskside and dayside auroral ovals and the DDA at noon, respectively. The three peaks were also seen in DMSP proton energy flux (thin line in Figure 9c) at nearly the same positions. Such excellent agreement on locations of the DDA and the auroral oval provides direct evidence that the DDA was composed mainly of precipitating protons. Note that the SI-12 counts of the three major peaks are roughly proportional to DMSP proton energy fluxes. The average proton energies corresponding to the three major peaks in Figure 9c are around 15 keV, 8 keV, and 15 keV (see Figure 10). The three peak SI-12 counts (after subtracting background levels) are about 16, 9, and 10, respectively. Using the results from *Gerard et*

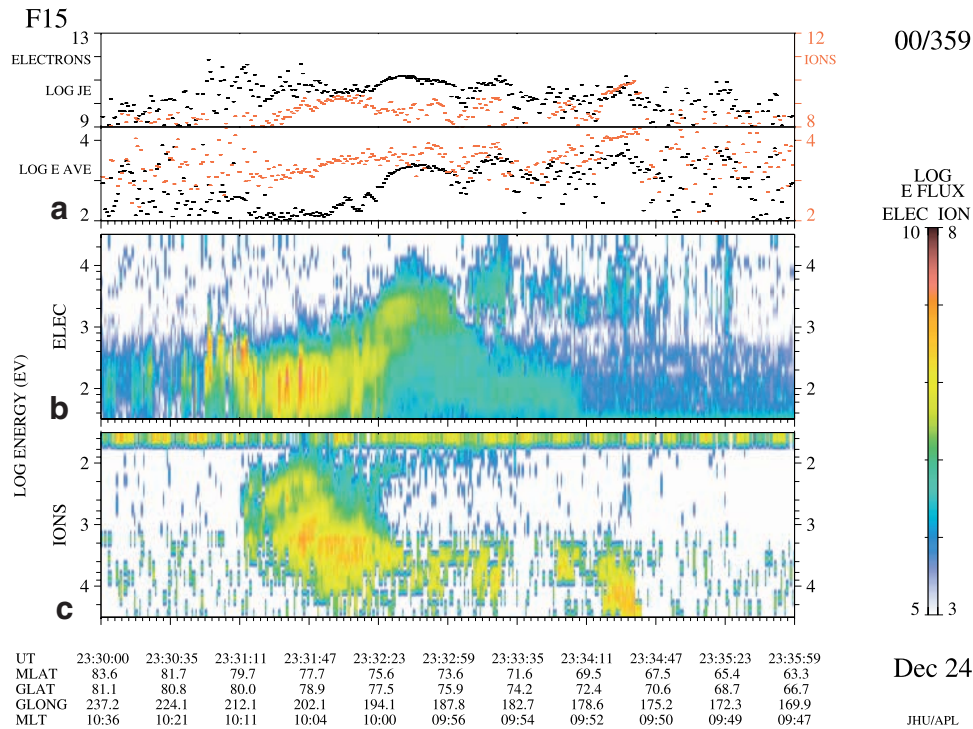


**Figure 7.** DMSP F15 precipitated particle data between 2330 and 2336 UT, 24 December 2000. (a) Total energy flux (ergs/cm<sup>2</sup>/s) of electrons (black) and ions (red). (b) Average energy (eV) of electrons and ions. (c) Electron differential energy flux. (d) Ion differential energy flux.

*al.* [2001], we estimated proton energy fluxes (using the count rate for 8 keV protons) as 0.53 (16.0/30.), 0.3 (9./30.), and 0.33 (10./30.) ergs/cm<sup>2</sup>/s, respectively. These values are also above but comparable to the DMSP measurements (0.42, 0.154, and 0.12 ergs/cm<sup>2</sup>/s).

[16] More details of precipitating protons and electrons are shown in Figure 10. Around 1408:24 UT, when the DMSP satellite passed the dayside auroral oval, the energy flux of electrons (black dots in the top panel of Figure 10) and protons (red dots) peaked at a same location. However, at the dayside subauroral oval latitudes the DMSP first detected electron energy flux peak around 1409:59 UT then the proton energy flux peak 1 minute later (around 1410:59 UT). The peak electron energy flux at 1409:59 UT (which is much higher than the peak proton energy flux at 1410:59 UT) corresponds to a minimum value of the SI-12 counts (between the dayside auroral oval peak and DDA peak, see Figure 9c). This indicates that electron precipitation has little or no contribution in the SI-12 intensities. Again, the DDA was solely due to energetic (>10 keV) proton precipitation. Though energetic electrons (around 10 keV) were also associated with the DDA, they cannot produce Doppler-shifted Lyman alpha emissions which would be detected by the SI-12. Certainly, they can produce emissions at other wavelengths, such as 130.4 nm, and 135.6 nm. These emissions are hard to detect owing to very bright dayglow. It is interesting to mention that the precipitated electrons in the dayside auroral oval have lower energy (<600 eV). However, the energy of precipitated protons in the dayside oval (between 1406:59 and 1408:59 UT) extended from 200 eV to >30 keV. Figure 10 also shows that there was basically no proton precipitation between

1409 and 1410 UT. This indicated that the DDA was clearly separated from the dayside auroral oval.

## 6. Discussion

[17] IMAGE SI-12 measurements indicate that DDA usually are located at subauroral latitudes (at or below

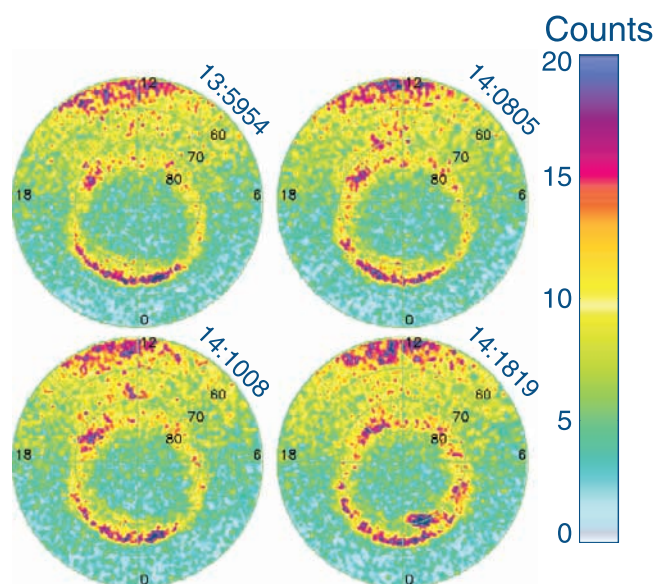


**Figure 8.** Similar to Figure 1 but for 28 December 2000. The persistent feature in dayside below 60 degree of magnetic latitude was again due to a leak of geocorona.



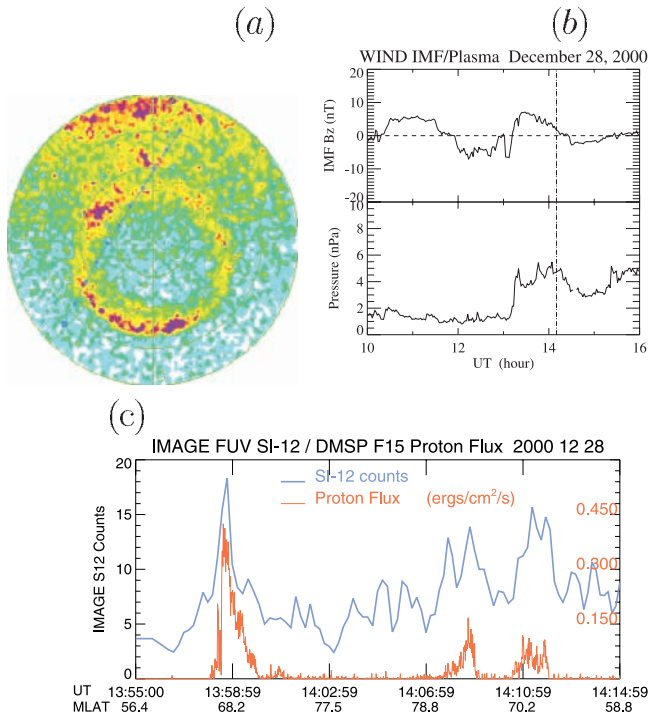


**Figure 9.** The same as Figure 6 but for 28 December 2000. The time of SI-12 image in Figure 9a is 1410:08 UT. The time interval in Figure 9c is between 1355 and 1415 UT.

70° magnetic latitude,  $L \leq 9$ , assuming dipole field) in the dayside. They are apparently triggered by sudden solar wind dynamic pressure enhancements when IMF  $B_z$  was northward. DDA are also short-lived with a lifetime of only  $\sim 10$  minutes. The analyzed events indicate that DDA could take form of “arc” or “patch.” As the SI-12 instrument measures Doppler-shifted (red shift) Lyman alpha, DDA seen by SI-12 must be due to energetic proton precipitation. Simultaneous DMSP particle observations confirm that DDA is composed mainly of protons with energy around and above 10 keV. Energetic (2–20 keV) electron precipitation was also detected with the DDA. This suggests that DDA could be observed by IMAGE WIC, SI-13, or other FUV instruments. However, strong FUV dayglow emissions at DDA locations make it difficult to detect DDA against the bright dayglow emissions seen at other wavelengths. Both the IMAGE and DMSP data confirm that DDA are separated from the dayside auroral oval; thus DDA do not share the same particle source with the dayside oval. All these facts suggest that the particle source of DDA is very likely in the dayside ring current, which is located in region of  $L = 2 \sim 9$ . The ring current is mainly carried by 10–100 keV protons [Daglis *et al.*, 1999]. On the basis of 3 years of equatorial proton data at 90° pitch angle from the Charge-Energy-Mass instrument on board the AMPTE/CCE satellite, Milillo *et al.* [2001] recently reported that for  $L$  between 6 and 9, corresponding on the Earth’s surface to the latitudes where the DDA are observed (65.9–70.5 MLAT), the proton fluxes for energies under a few tens of keV increase with  $L$ . Furthermore, their empirical model shows that the energy peak in the

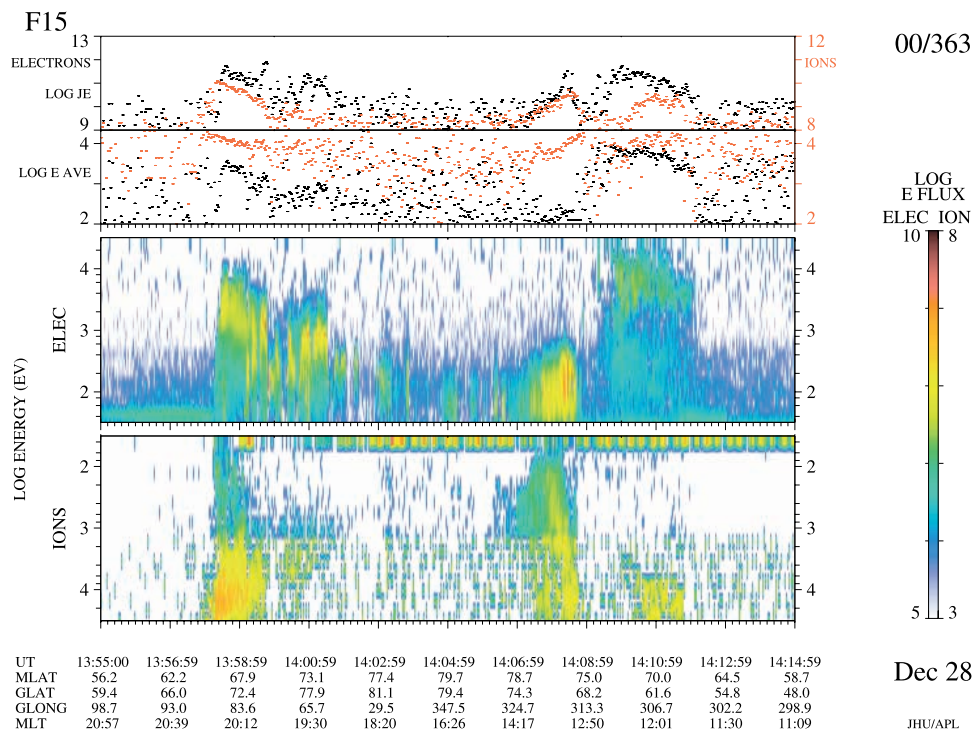


**Figure 10.** The same as Figure 7 but for DMSP data between 1355 and 1415 UT, 28 December 2000.

dayside is around or above 10 keV. (For details, see Figure 2 of Milillo *et al.* [2001]). These measurements indicate that energy of major proton flux in the  $L = 6-9$  ( $65.9^\circ-70.5^\circ$  MLAT) range is of  $\sim 10$  keV or above. Such a result is consistent with the IMAGE and DMSP observations that there are existing energetic proton fluxes in the inner magnetosphere. Zhou and Tsurutani [1999] proposed a model/mechanism to explain brightening of the dayside auroral oval following fast interplanetary shocks. Such an explanation also applies to DDA. Solar wind with sudden enhanced dynamic pressure first compresses the magnetopause nose at  $\sim 12$  MLT. Assuming that the first adiabatic invariant of trapped plasma is conserved, compression of the magnetospheric magnetic field leads to an increase in the perpendicular kinetic energy of protons and electrons on those field lines. The enhanced temperature anisotropy of the proton/electron distribution function will result in cyclotron instability. The growth of electromagnetic ion cyclotron and whistler mode waves leads to enhanced proton/electron pitch angle scattering, filling of the particle loss cone, and results in proton/electron loss into the upper ionosphere. As significant compression can only occur on the dayside, major proton/electron precipitation will be on the dayside, around 1200 MLT. Orientation of IMF  $B_y$  or IMF clock angle may cause DDA to shift its location in the dawn-dusk direction. We will examine this in greater detail in a future work. DDA were observed mostly under northward IMF conditions. This is because northward IMF allows solar wind pressure to effectively compress the magnetopause. Because of northward IMF, a very small fraction of the solar wind particles enter the magnetosphere. Once protons/electrons in the dayside ring current have precipitated into the atmosphere, they cannot be replaced quickly by protons/electrons from the nightside magnetosphere, as it takes 5–6 hours for 13 keV protons to drift from the nightside to the dayside magnetosphere at an altitude of 6.6 Re [Roederer, 1970]. This may explain why the DDA are usually very dynamic and short-lived. The third solar wind pressure enhancement on 8 November 2000 occurred  $\sim 2$  hours or less after the second enhancement, possibly before the particle populations could be replenished. This line of reasoning is also supported by fact that the auroral oval was extremely weak before the third solar wind pressure enhancement arrived, indicating very weak proton/electron flux in the dayside inner magnetosphere or ring current. There may still be a DDA following the third pressure enhancement; it was just too weak to detect. It is interesting to note that there was one DDA case occurred during southward IMF on 28 October 2000. This DDA was extremely short-lived with a lifetime only  $\sim 4$  minutes. More such cases are needed to study the differences/similarities between them and DDA under northward IMF.

## 7. Summary

[18] The IMAGE SI-12 observations show that the dayside detached auroras were caused by sudden solar wind dynamic pressure enhancements. It is also found that northward IMF is a necessary condition for DDA to occur (in all but one case of the 25 examples seen in year 2000 data, IMF  $B_z$  is northward). Simultaneous observations by DMSP

particle detectors confirm that the dayside detached auroras seen by IMAGE SI-12 were caused by energetic ( $>10$  keV) precipitating protons. Occurrence of DDA can be well explained by a model proposed by Zhou and Tsurutani [1999] that solar wind dynamic pressure enhancements caused increase of proton's/electron's temperature anisotropy leading to cyclotron instability which diffused protons/electrons into a loss cone. Short lifetime of DDA may be due to slow replacement of precipitated protons/electrons from the nightside magnetosphere under northward IMF condition. Both electrons and protons have the same energy range, indicating no field-aligned acceleration. This further confirms that the precipitated protons/electrons were due to wave scattering.

[19] Quantitative relationship between SI-12 intensities and proton energy fluxes need further study by using auroral models, such as B3C auroral model [Daniell, 1993] and SI-12 response function. More cases will be examined for possible dependence of DDA brightness and location on magnitude of solar wind dynamic pressure enhancements and orientation of IMF  $B_y$ .

[20] **Acknowledgments.** DMSP particle data were obtained from Pat Newell and provided by Fred Rich (AFRL). Solar wind IMF/Plasma data are from [http://cdaweb.gsfc.nasa.gov/cdaweb/istp\\_public/](http://cdaweb.gsfc.nasa.gov/cdaweb/istp_public/). We thank Kan Liu and Shin-ichi Ohtani for their discussions.

[21] Arthur Richmond thanks Robert A. Hoffman and Anna Milillo for their assistance in evaluating this manuscript.

## References

- Anger, C. D., M. C. Moshupi, D. D. Wallis, J. S. Murphree, L. H. Brace, and G. G. Shepherd, Detached auroral arcs in the trough region, *J. Geophys. Res.*, **83**, 2583, 1978.
- Burch, J. L., Image mission overview, *Space Sci. Rev.*, **91**, 1, 2000.
- Daglis, I. A., W. Baumjohann, and S. Orsini, The terrestrial ring current: Origin, formation and decay, *Rev. Geophys.*, **37**, 407, 1999.
- Daniell, R. E., Jr., Modeling of optical signatures of electron spectra in the ionospheric heating experiments, *Proc. Progr. 7th Int. Ionospheric Effects Symp.*, SRI-Int, Arlington, Va., 1993.
- Fuselier, S. A., J. L. Burch, S. B. Mende, T. E. Moore, C. J. Pollock, B. W. Reinish, and B. R. Sandel, Multi-instrument observations from IMAGE, *EOS Trans. AGU*, **81**, Fall Meet. Suppl., Abstract SM71B-03, 2000.
- Fuselier, S. A., et al., Ion outflow observed by IMAGE: Implications for source regions and heating mechanisms, *Geophys. Res. Lett.*, **28**, 1163, 2001.
- Gerard, J.-C., B. Hurbert, M. Meurant, V. I. Shematovich, D. V. Bisikalo, H. Frey, S. Mende, G. R. Gladstone, and C. W. Carlson, Observation of the proton aurora with IMAGE FUV imager and simultaneous ion flux in situ measurements, *J. Geophys. Res.*, **106**, 28,939, 2001.
- Hardy, D. A., L. K. Schmitt, M. S. Gussenhoven, F. J. Marshall, H. C. Yeh, T. L. Shumaker, A. Ube, and J. Pantazis, Precipitating electron and ion detectors (SSJ/4) for the block 5D/flights 6-10 DMSP satellite: Calibration and data presentation, *Rep. AFGL-TR-84-0317*, Air Force Geophys. Lab., Hanscom Air Force Base, Mass., 1984.
- Immel, T. J., et al., Precipitation of auroral protons in detached arcs, *Geophys. Res. Lett.*, accepted, 2002.
- Mende, S. B., et al., Far ultraviolet imaging from the IMAGE spacecraft, 3, Spectral imaging of Lyman alpha and OI 135.6 nm, *Space Sci. Rev.*, **91**, 287, 2000.
- Milillo, A., S. Orsini, and I. A. Daglis, Empirical model of proton fluxes in the equatorial inner magnetosphere: Development, *J. Geophys. Res.*, **106**, 25,713, 2001.
- Moshupi, M. C., L. L. Cogger, D. D. Wallis, J. S. Murphree, and C. D. Anger, Auroral patches in the vicinity of the plasmopause, *Geophys. Res. Lett.*, **4**, 37, 1977.
- Newell, P. T., Reconsidering the inverted-V particle signature: Relative frequency of large-scale electron acceleration events, *J. Geophys. Res.*, **105**, 15,779, 2000.
- Roederer, J. G., *Dynamics of Geomagnetically Trapped Radiation*, Springer-Verlag, New York, 1970.

- Vondrak, R., S. Harris, and S. Mende, Groundbased observations of sub-auroral energetic-electron arcs, *Geophys. Res. Lett.*, *10*, 557, 1983a.
- Vondrak, R. R., J. S. Murphree, C. D. Anger, and D. D. Wallis, Ionospheric characteristics of a detached arc in the evening-sector trough, *Geophys. Res. Lett.*, *10*, 561, 1983b.
- Wallis, D. D., J. R. Burrows, M. C. Moshupi, C. D. Anger, and J. S. Murphree, Observations of particle precipitating into detached arcs and patches equatorward of the auroral oval, *J. Geophys. Res.*, *84*, 1347, 1979.
- Zhang, Y., L. Paxton, and T. Immel, Sudden enhancement of solar wind dynamic pressure and dayside detached aurora, *Eos Trans. AGU*, Fall Meet. Suppl., Abstract SM41B-0814, 2001.
- Zhou, X., and B. T. Tsurutani, Rapid intensification and propagation of the dayside aurora: Large-scale interplanetary pressure pulses (fast shock), *Geophys. Res. Lett.*, *26*, 1097, 1999.
- 
- H. U. Frey, T. J. Immel, and S. B. Mende, Space Science Laboratory, University of California, Berkeley, CA 94720-7450, USA. (hfrey@ssl.berkeley.edu; immel@ssl.berkeley.edu; mende@ssl.berkeley.edu)
- L. J. Paxton and Y. Zhang, Space Department, Johns Hopkins University Applied Physics Laboratory, 11100 Johns Hopkins Road, Laurel, MD 20723, USA. (larry.paxton@jhuapl.edu; yongliang.zhang@jhuapl.edu)